

## RESEARCH ARTICLE

# Low Velocity Impact Response of Syntactic Foams Reinforced with Varying Volume Fractions of Cenosphere and Rubber Crumb

Vishwas Mahesh

Department of Industrial Engineering and Management, Siddaganga Institute of Technology, Tumakuru 572103, Visvesvaraya Technological University, Belagavi, Karnataka, India

**ABSTRACT** – Syntactic foams reinforced with industrial waste-derived cenospheres and rubber crumb fillers present a promising pathway for developing lightweight, impact-resistant materials. However, a comprehensive comparison of their energy absorption characteristics under low velocity impact (LVI) loading remains underexplored. This study investigates the LVI response of syntactic foams with varying volume fractions (20%, 40%, and 60%) of cenospheres (SFC) and rubber crumb (SFR), benchmarked against neat epoxy (NE). The key findings indicate that rubber crumb-reinforced foams (SFR60) exhibit the highest absorbed energy of 16.75 J at an impact energy of 118.82 J, surpassing the NE (6.46 J), indicating superior impact dissipation. Cenosphere-based foams (SFC60) achieve the highest specific energy absorption (SEA) of 0.0115 Jm<sup>3</sup>/kg, a 117% improvement over NE (0.0053 Jm<sup>3</sup>/kg), due to their lower density and increasing filler content from 20% to 60% significantly enhances both absorbed energy and SEA, with cenosphere-reinforced foams exhibiting higher efficiency per unit mass. These findings highlight the performance trade-offs between energy absorption capacity and material efficiency, providing valuable insights for designing sustainable syntactic foams for aerospace, automotive, and protective applications.

## ARTICLE HISTORY

Received : 29<sup>th</sup> Nov. 2024  
 Revised : 08<sup>th</sup> July 2025  
 Accepted : 10<sup>th</sup> Aug. 2025  
 Published : 18<sup>th</sup> Sept. 2025

## KEYWORDS

*Syntactic foams*  
*Cenosphere*  
*Rubber crumb*  
*Core material*  
*Low velocity impact*  
*Energy absorption*  
*Gradation test*

## 1. INTRODUCTION

The demand for lightweight, high-strength materials with excellent impact resistance is growing across various industries, particularly in aerospace, automotive, and marine applications [1]. Syntactic foams, which are composite materials typically consisting of hollow microspheres embedded in a polymer matrix, have gained significant attention due to their unique combination of low density and enhanced mechanical properties. These materials are designed to absorb and dissipate energy, making them ideal for applications requiring resistance to impact and other dynamic loads [2]. Particulate composites are often used as the core materials in composite sandwiches because they offer a robust and lightweight framework. Additionally, impact resistance, electrical properties, magnetic characteristics and damage tolerance can all be enhanced by adding reinforcing particle fillers to epoxies [3] - [7]. In lightweight applications such as aerospace construction, where weight reduction can lead to improved fuel efficiency and performance, particulate composites are particularly advantageous. Furthermore, due to their enhanced properties, particulate composites can also be used in applications such as packaging, where there is a risk of damage. Typically, two strong and rigid face sheets are sandwiched around a lightweight material to form the core of a sandwich structure. The core functions are to reduce weight while simultaneously enhancing the rigidity and strength of the sandwich structure [8], [9].

Achieving high specific compressive strength and bending stiffness in a sandwich construction can be accomplished by utilizing a particulate-filled composite material as the core. The lightweight core design reduces the overall weight of the structure, while the particle fillers enhance the mechanical properties of the composite material. Sandwich structures with particulate-filled composite cores are ideal for aerospace and other weight-sensitive applications where high performance is essential. Furthermore, the improved mechanical characteristics of the particulate-filled composite core provide increased resistance to impact and various types of damage, making them well-suited for use in harsh environments [10] - [12]. Many different types of particles are used as fillers in composite materials. The choice of filler material is determined by the desired properties of the composite. Fillers serve multiple functions, including reducing the overall cost of the final product and enhancing various properties to meet specific application requirements. Materials such as minerals, metals, ceramics, polymers, and industrial waste can all be utilized as polymer fillers [13] - [16].

The study on the low-velocity impact behavior of functionally graded, treated, and untreated cenosphere-based syntactic foams examines the impact resistance of syntactic foams in relation to the influence of functional gradation and surface treatment of cenospheres. The researchers developed functionally graded foams by varying the filler concentration through the thickness of the specimen, aiming to improve energy absorption and damage tolerance. Treated cenospheres, modified to enhance interfacial bonding with the matrix, were compared with untreated counterparts under low-velocity impact loading. The findings revealed that functionally graded syntactic foams with treated cenospheres exhibited superior impact resistance, reduced damage propagation, and better energy dissipation compared to their uniformly filled

or untreated counterparts. This study highlights the effectiveness of both particle surface treatment and gradient design in optimizing the mechanical performance of syntactic foams for impact-critical applications [2].

Recent advancements in cenosphere-reinforced syntactic foams have increasingly focused on enhancing specific strength to meet the demands of weight-sensitive structural applications. These foams, composed of hollow aluminosilicate microspheres embedded in a polymer matrix, offer an excellent balance of low density and mechanical performance. Researchers have explored various strategies to improve specific strength, such as optimizing cenosphere volume fractions, employing hybrid reinforcement with fibers or nanoparticles, and surface-treating cenospheres to improve interfacial adhesion. Studies have shown that incorporating cenospheres up to an optimal threshold significantly increases specific strength by reducing composite weight while maintaining or enhancing stiffness and load-bearing capacity. Additionally, advanced fabrication techniques, such as functionally graded layering and controlled filler dispersion, have further enhanced the strength-to-weight ratio. These developments position cenosphere-based syntactic foams as promising candidates for lightweight structural components in aerospace, automotive, and marine sectors, where high specific strength is critical [17].

A study examining the effects of reinforcement using both waste glass and barley straw on the water resistance, mechanical, and thermal properties of polyethylene composites presents a sustainable approach to composite development by utilizing agricultural and industrial waste as reinforcement in a polyethylene matrix. The dual inclusion of waste glass fibers and barley straw aimed to balance the mechanical performance and environmental impact of the resulting composites. The findings demonstrated that waste glass improved the stiffness and tensile strength of the composites, while barley straw contributed to reduced density and enhanced biodegradability. The hybrid reinforcement also significantly influenced thermal stability and water absorption behavior, with the treated fibers showing better interfacial bonding and reduced moisture uptake. Overall, the study highlights the potential of combining organic and inorganic waste reinforcements to produce environmentally friendly composites with competitive mechanical and thermal properties, suitable for lightweight structural and semi-structural applications [18].

The study on the effect of alkaline treatment on the thermal and mechanical properties of sugar palm fiber-reinforced thermoplastic polyurethane composites investigates the influence of surface modification on the performance of natural fiber-reinforced polymer composites. Alkaline treatment (typically using NaOH) was applied to sugar palm fibers to remove impurities, waxes, and non-cellulosic components, thereby improving fiber-matrix adhesion. The results revealed that treated fibers led to enhanced mechanical properties, including increased tensile strength and modulus, due to better stress transfer at the interface. Thermal analysis showed improved thermal stability of the composites with treated fibers, attributed to cleaner fiber surfaces and stronger interfacial bonding. Moreover, the treatment reduced moisture absorption, enhancing dimensional stability. This study underscores the importance of chemical treatment in improving the compatibility of natural fibers with polymer matrices like thermoplastic polyurethane (TPU), making such composites more viable for structural and semi-structural applications in automotive and consumer industries [19].

The primary criterion for material selection is the required functionality of the composite. Since the morphology of filler particles significantly influences the properties of the composite, particles are often classified based on their shape. The most common morphologies include flaky, fibrous, spherical, cubical, and block-like forms. The size of the interfacial zone between the particle and the matrix resin is affected by differences in surface area among these shapes for a given volume. Each geometry exhibits a distinct stress concentration factor due to variations in aspect ratio and corner radius of curvature [20], [21]. Fillers with spherical particles are more commonly used than those with other shapes. The use of cenospheres, hollow spherical particles, in the production of low-density, highly damage-tolerant core materials has increased significantly in recent years. These low-density materials are classified as near-cell-structured foams and are commonly referred to as "syntactic foams." The density or composition of cenospheres can be tailored to customize the density of syntactic foams across a wide range [22], [23].

Recent advancements in syntactic foam technology have focused on enhancing its energy absorption capabilities through the incorporation of various types of fillers. Filler-reinforced composites represent a class of advanced materials in which a matrix, typically a polymer, is reinforced with filler materials such as nanoparticles, fibers, or particulates. These fillers play a crucial role in improving the mechanical, thermal, and electrical properties of the composite, providing a synergistic effect that exceeds the performance of the individual components [24], [25]. By strategically incorporating fillers into the matrix, filler-reinforced composites can be engineered to achieve tailored properties such as increased strength, stiffness, toughness, and wear resistance, while maintaining or even reducing the overall weight. Furthermore, the type, size, shape, and concentration of fillers can be precisely adjusted to meet specific performance requirements and application needs across a wide range of industries, including automotive, aerospace, electronics, and biomedical engineering [26], [27]. The development and optimization of filler-reinforced composites remain a central focus of research, driving innovations in material design, processing techniques, and applications. These advancements hold the potential to revolutionize various technological sectors while addressing critical challenges related to sustainability and performance [28], [29].

Rubber crumb particles, derived from recycled tires, represent an innovative approach to enhancing the impact resistance of syntactic foams. These highly elastic particles can undergo significant deformation under stress, effectively absorbing and dissipating energy through hysteresis [30]. When embedded in a polymer matrix, rubber crumbs create localized regions of high deformability, further enhancing the composite's capacity to absorb impact energy [6], [31].

Despite extensive research on syntactic foams, particularly those reinforced with cenospheres, a notable lack of comparative studies remains to evaluate their low-velocity impact performance against alternative reinforcements, such as rubber crumb. While cenosphere-reinforced foams are well recognized for their lightweight and strength characteristics, the impact resistance of rubber crumb-reinforced syntactic foams, especially under low-velocity conditions, has not been adequately explored. Furthermore, direct comparisons between these two reinforcement types under identical testing protocols are scarce, making it difficult to understand the distinct roles they play in energy absorption, damage tolerance, and overall mechanical behavior.

To address this gap, the present study aims to perform a systematic comparative assessment of cenosphere and rubber crumb-reinforced syntactic foams under low-velocity impact loading. By evaluating and comparing their energy absorption capabilities, peak and critical force responses, and failure mechanisms, this work aims to provide deeper insights into material selection for impact-critical applications in the aerospace, automotive, and marine sectors. The outcomes of this study are expected to guide material design choices where optimized impact resistance is essential.

## 2. METHODS AND MATERIALS

### 2.1 Materials

In order to develop the syntactic foams in this work, rubber crumb of grade CRMB60, obtained from SM enterprises, Bengaluru, Karnataka, India and cenosphere of grade CIL 100, obtained from Cenosphere India Pvt. Ltd., Kolkata, West Bengal, India, are used as fillers in the epoxy-based matrix Lapox L12, coupled with K6 hardener. The components used in the development of syntactic foams are shown in Figure 1.



Figure 1. Raw materials utilized for production of syntactic foams: (a) cenosphere; (b) rubber crumb; (c) epoxy matrix

### 2.2 Methods

Syntactic foams are fabricated by mixing resin at room temperature with a specified volume percentage of cenospheres or rubber crumb. After the components are blended, 10% hardener (in a 1:10 ratio) is added to the mixture, which is then degassed to remove entrapped air before being poured into aluminum molds. This process results in a uniform and consistent slurry. The cast slabs are allowed to cure at room temperature for 24 hours. Three distinct syntactic foams are prepared using cenosphere/rubber crumb concentrations of 20%, 40%, and 60% in an epoxy matrix. Additionally, virgin specimens, those without any matrix filler, are prepared for comparison. The methodology used to fabricate the proposed syntactic foams is illustrated in Figure 2.



Figure 2. Steps involved in preparation of syntactic foams

The produced composites and their designations are displayed in Table 1. The fabricated laminates are shown in Figure 3. Specimens required for the various tests conducted in this study were cut from the resultant laminates in accordance with the relevant ASTM standards. The uniform dispersion of rubber crumb and cenosphere particles within the epoxy matrix is illustrated in Figure 4.

Table 1. Syntactic foams and their designations

Syntactic Foam	Designation
Neat Epoxy	NE
20 Vol% Cenosphere reinforced in Epoxy	SFC20
40 Vol% Cenosphere reinforced in Epoxy	SFC40
60 Vol% Cenosphere reinforced in Epoxy	SFC60
20 Vol% Rubber Crumb reinforced in Epoxy	SFR20
40 Vol% Rubber Crumb reinforced in Epoxy	SFR40
60 Vol% Rubber Crumb reinforced in Epoxy	SFR60

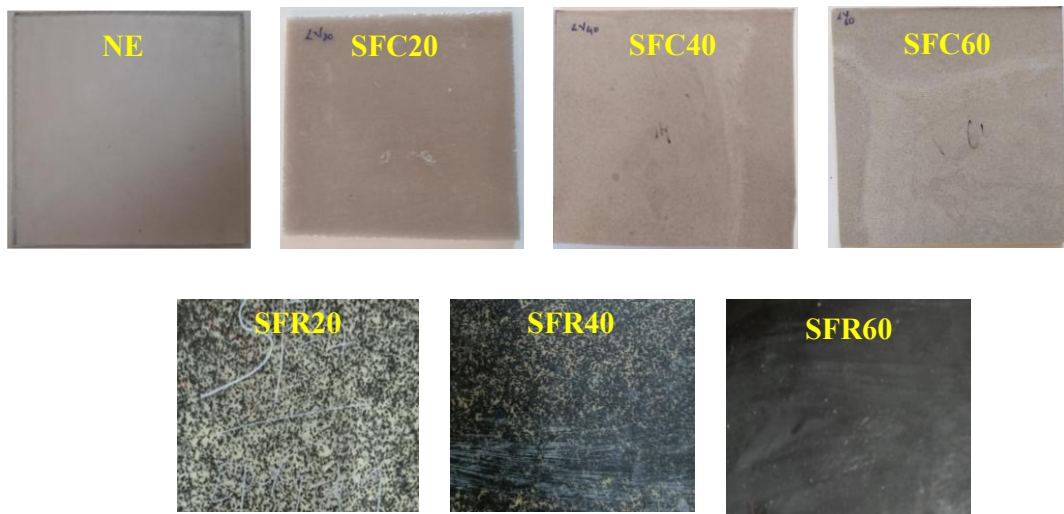


Figure 3. Obtained laminates of neat epoxy and syntactic foams

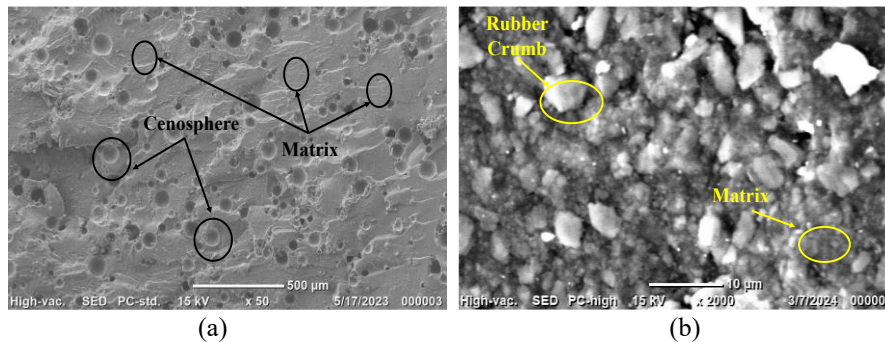


Figure 4. Uniform distribution of (a) cenosphere and (b) rubber crumb in epoxy matrix

The density of the developed composites was calculated using Eq. 1. The obtained density is used to calculate specific energy absorption (SEA).

$$\rho = \frac{mass}{volume} \tag{1}$$

### 2.3 Gradation Test

Cenospheres are composed of a range of solid, hollow, and composite particles, typically exhibiting a spherical shape. While cenospheres are hollow fly ash particles, plerospheres are composite particles consisting of smaller solid particles enclosed within a hollow spherical shell. Due to their varying densities, cenosphere particles tend to rise to the surface when mixed with epoxy and poured, leading to gradation in the prepared specimens. This gradation occurs as the cenosphere concentration decreases with depth, resulting in a higher epoxy content and increased weight at the bottom, and lower weight at the top. Figure 5(a) illustrates the functional gradation (FG) schematic of a cenosphere-based core

sample. Dispersing rubber crumb into an epoxy matrix yields a type of rubber-toughened composite, which enhances the material's toughness and impact resistance. The natural settling tendency of denser rubber crumb particles during the curing process can be leveraged to create a functionally graded material (FGM), in which the bottom layer contains a higher concentration of rubber crumb and the top layer contains a lower concentration. Figure 5(b) shows the schematic of the rubber crumb-based core.

A syntactic foam specimen with dimensions of 10 × 10 × 10 mm was fabricated for each configuration. This was then sectioned into four equal slices (10 × 10 × 2.5 mm) along the vertical axis. Each slice was weighed, followed by thermal treatment in an electric Bunsen furnace until the organic matrix was fully combusted, leaving behind the inorganic fly ash/rubber crumb content. The residual weight was recorded, and the fly ash/rubber crumb weight fraction in each layer was calculated using Equation 2. This method enabled a quantitative assessment of filler distribution across the specimen's height. This procedure was designed based on methodologies adapted from related literature and was implemented to maintain consistency and reproducibility [32].

$$\text{Weight of Filler} = \left( \frac{\text{Weight of Residue}}{\text{Weight of sample}} \right) \tag{2}$$

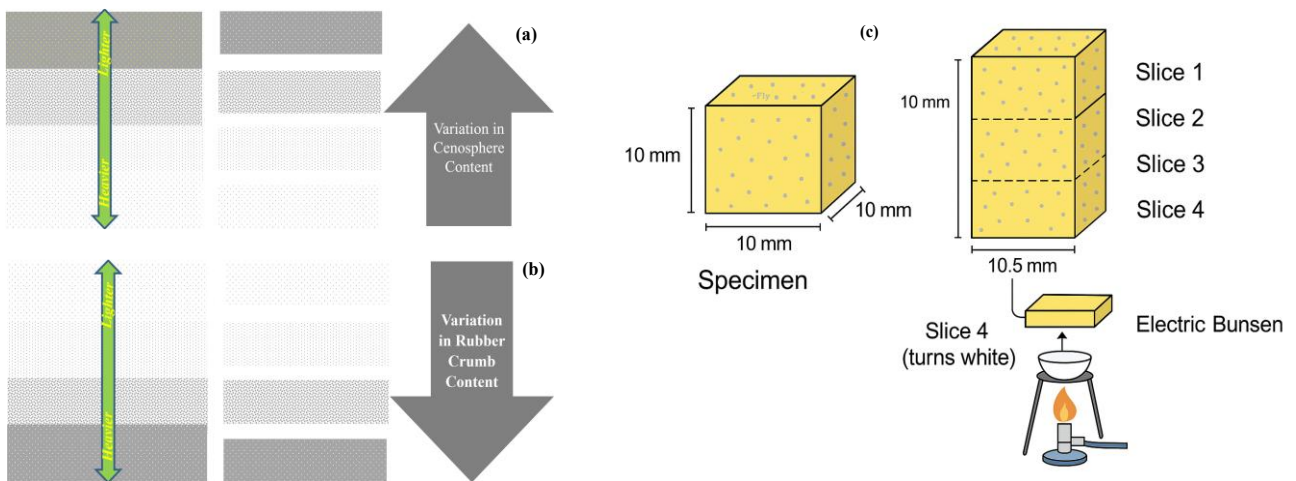


Figure 5. Schematic representation of gradation in (a) cenosphere; (b) rubber crumb-based cores and (c) procedure of gradation test

### 2.4 Low Velocity Impact

As shown in Figure 6, the energy absorption capacities of the proposed syntactic foams were evaluated using a low-velocity impact (LVI) test conducted with a drop-weight impact tester and a hemispherical impactor, following the ASTM D7136 standard. The specimen size was 150 mm × 150 mm. For each testing condition, three samples were tested, and the average value was reported as the result.

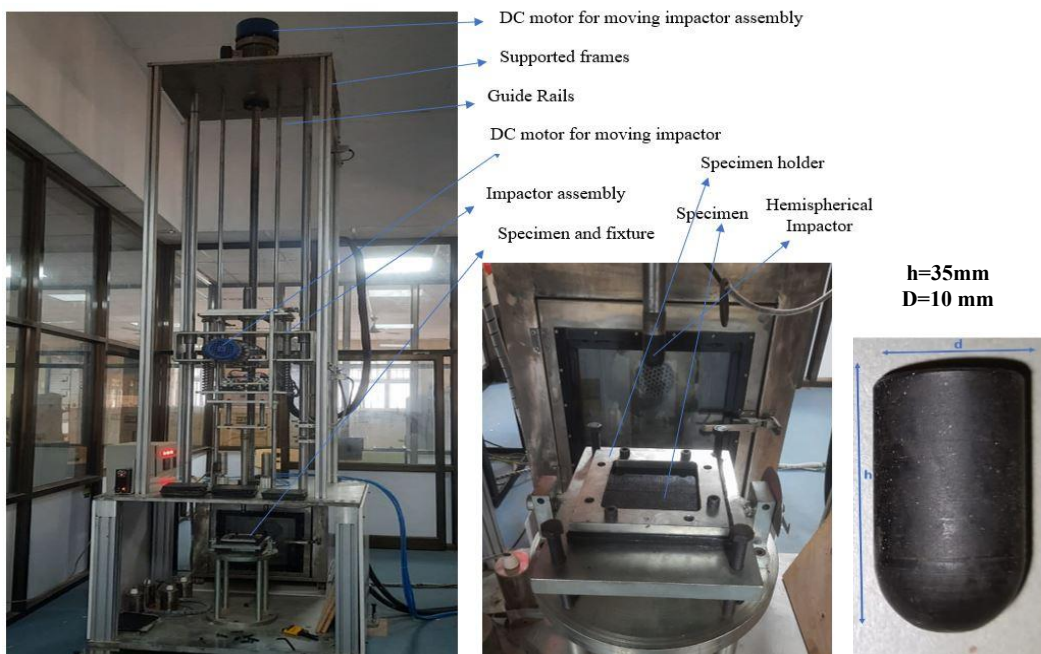


Figure 6. Set up used to perform drop weight impact testing

The weight of the impactor assembly is 8.09 kg. The drop height is set to 0.5 m, 1 m, and 1.5 m, which corresponds to impact velocities of 3.13 m/s, 4.42 m/s, and 5.42 m/s during impact testing utilizing specimens in the specimen holder of the impact machine. Thus, the relative impact energies are 39.62 J, 79.02 J, and 118.82 J. The experiment was conducted at room temperature. To get the various impact energies, the impactor's drop height was altered. As the drop height rises, so does the energy held within the impactor.

The impact velocities and impact energies are calculated using Eq. 3 and Eq. 4, respectively.

$$v_i = \sqrt{2gh} \quad (3)$$

$$E_i = \frac{1}{2}mv_i^2 \quad (4)$$

where,  $v_i$  is the impact velocity in m/s,  $g$  is the acceleration due to gravity ( $9.81 \text{ m/s}^2$ ) and  $h$  is the drop height in m,  $m$  is the mass of the impactor in Kg (8.09 kg),  $E_i$  is the impact energy in Joules.

### 3. RESULTS AND DISCUSSIONS

#### 3.1 Gradation Test

Utilizing the weight approach on the FG core, gradation characterization is achieved. The variation of weight in each layer of foams is presented in Figures 7(a) and 7(b) for cenosphere and rubber crumb particles, respectively.

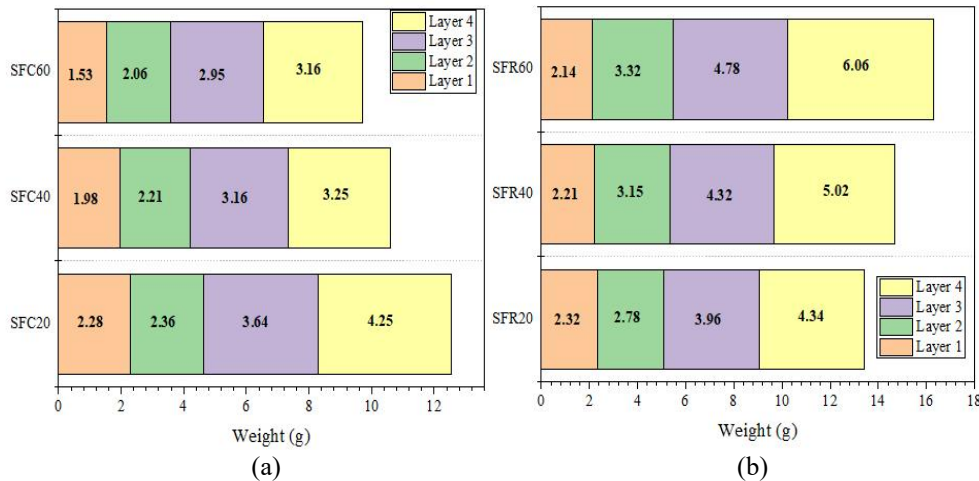


Figure 7. Gradation establishment in syntactic foams reinforced with (a) cenosphere and (b) rubber crumb

As the cenosphere content increases from SFC20 to SFC60, the total weight of the syntactic foam decreases. This is expected because cenospheres are hollow particles with a lower density, reducing the overall weight of the composite. Similar trends have been reported by Doddamani et. al.[32] where increased cenosphere content led to a reduction in density and overall weight, enhancing the specific strength and buoyancy of syntactic foams. For SFC20, the top layers (Layer 1 and 2) contribute 36.9% of the total weight, while the bottom layers (Layer 3 and 4) contribute 63.97%. In SFC40, the weight distribution shifts slightly towards the bottom layers (Layer 3 and 4), contributing 60.47%, while the top layers (Layer 1 and 2) contribute 39.53%. SFC60 has the most pronounced weight distribution towards the lower layers, with the bottom layers (Layer 3 and 4) contributing 63%, and the top layers (Layer 1 and 2) making up 37%. This gradient effect is consistent with findings by Rohatgi et al. [33], who observed particle sedimentation in aluminum matrix syntactic foams depending on particle density and viscosity of the matrix. However, unlike high-density fillers, cenospheres, due to their low density, are less prone to significant settling, which aligns with our observed marginal weight variation in SFC foams.

In the case of syntactic foam with rubber crumb particles, the weight increases consistently from Layer 1 to Layer 4, with a gradual but noticeable jump between layers. This indicates that, at 20% rubber crumb content, the material tends to settle more toward the bottom layers, but there is still a moderate distribution of the rubber crumbs throughout the foam. The difference in weight between Layer 1 and Layer 4 is approximately 2.02 grams, showing that while there is some settling, the gradation is not overly steep. This suggests that at lower rubber crumb content (20%), the matrix remains relatively homogenous, and the rubber particles are not excessively settling toward the bottom. In the case of SFR40, there is a more pronounced weight increase between the layers compared to SFR20. The jump between Layer 1 and Layer 2 is significant (0.94 grams), and the weight continues to increase steeply through Layer 3 and Layer 4. The difference between Layer 1 and Layer 4 is now 2.81 grams, a larger gradient than in SFR20. This suggests that with 40% rubber crumb content, the particles tend to settle more toward the bottom layers during curing. The higher content of rubber crumbs likely enhances the gravitational settling, leading to a bottom-heavy structure where the lower layers are significantly denser. SFR60 shows the most dramatic increase in weight from Layer 1 to Layer 4. The jump from Layer

1 to Layer 2 is 1.18 grams, which is the largest gap so far, and the difference between Layer 3 and Layer 4 (1.28 grams) is also substantial. The overall difference between Layer 1 and Layer 4 is 3.92 grams, indicating that the rubber crumb particles are predominantly concentrated in the bottom layers. At 60% rubber crumb content, the matrix shows significant gradation, with the top layers remaining relatively lighter and the bottom layers becoming heavily reinforced and much denser. The stronger gravitational settling at higher crumb content can be attributed to increased particle agglomeration and delayed gelation of the resin, as similarly observed in the work of Zhao et al. [34], who noted that at higher filler loadings, rubber particles tend to sink more rapidly unless strong particle–matrix interfacial bonding or thixotropic agents are used to suspend them. This illustrates that as the rubber crumb percentage increases, the material becomes increasingly bottom-heavy, with greater amounts of rubber crumbs settling in the lower layers due to their density and the slower curing time allowing them to sink.

### 3.2 Impact Energy Absorption

During an impact event, a portion of the overall impact energy is dissipated by the specimen through the creation of damage. This dissipated portion is referred to as the absorbed energy. At the moment of contact ( $t = 0$  s), the impactor transfers its kinetic energy to the specimen. Part of this energy is temporarily stored as elastic deformation, while the remainder is primarily lost due to damage formation, with minor losses occurring through friction, sound, and heat. Once the impactor's entire kinetic energy is transferred, it is converted into elastic strain energy stored in the specimen. This stored energy is then partially returned to the impactor until separation occurs, after which the load–time curve shows a descending trend [35]. The proposed syntactic foams were subjected to low-velocity impact (LVI) testing at varying impact velocities of 3.13 m/s, 4.42 m/s, and 5.42 m/s, corresponding to impact energies of 39.62 J, 79.02 J, and 118.82 J, respectively. Table 2 summarizes the impact characteristics of the syntactic foams under the specified conditions.

Table 2. Energy absorption of syntactic foams

Syntactic foams	Energy (J)			Density (kg/m <sup>3</sup> )	Specific Energy Absorption (SEA) in Jm <sup>3</sup> /kg
	Impact	Elastic	Absorbed		
NE	39.62	37.86	1.76	1210	0.0015
	79.02	74.25	4.77		0.0039
	118.82	112.36	6.46		0.0053
SFC20	39.62	36.81	2.81	1115	0.0025
	79.02	73.65	5.37		0.0048
	118.82	111.75	7.07		0.0063
SFR20	39.62	36.50	3.12	1530	0.0020
	79.02	72.80	6.22		0.0041
	118.82	109.37	9.45		0.0062
SFC40	39.62	36.32	3.30	1030	0.0032
	79.02	72.67	6.35		0.0062
	118.82	107.50	11.32		0.0110
SFR40	39.62	36.06	3.56	1580	0.0023
	79.02	71.94	7.08		0.0045
	118.82	104.84	13.98		0.0088
SFC60	39.62	36.31	3.31	1005	0.0033
	79.02	68.29	10.73		0.0107
	118.82	107.28	11.54		0.0115
SFR60	39.62	35.44	4.18	1630	0.0026
	79.02	66.59	12.43		0.0076
	118.82	102.07	16.75		0.0103

The energy absorption behavior of the developed syntactic foams at different levels of impact energy is presented in Figure 8(a). Each configuration, under each testing condition, is tested in triplicate. The neat epoxy samples show the lowest energy absorption, with values of 1.76 J, 4.77 J, and 6.46 J at the three respective energy levels. The primary reason for this low energy absorption is the homogeneous nature of the epoxy matrix, which lacks the microstructural elements necessary for effective energy dissipation. Epoxy, being a brittle polymer, tends to fracture and fail without significant deformation, resulting in limited energy absorption capacity. This is consistent with the findings of Mahesh et al. [36]. Introducing 20% filler content increases energy absorption both in the case of cenosphere and rubber crumb bases SFs. SFC20 absorbs 2.81 J, 5.37 J, and 7.07 J, while SFR20 shows an enhanced ability to absorb energy by 11%-33.66%. Rubber crumbs, being more deformable than cenospheres, provide better energy dissipation through their ability to undergo higher levels of elastic and plastic deformation. This results in improved energy absorption ranging from 11% to 33.66% compared to SFC20.

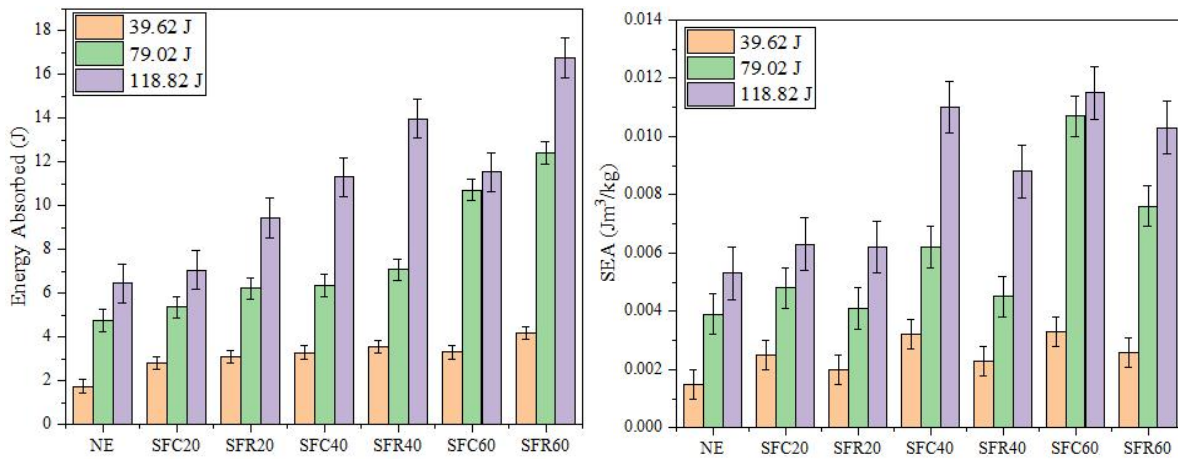


Figure 8. (a) Energy absorption and (b) SEA of developed syntactic foams at various energy levels

The improvement in SFC20 is attributed to the presence of low-density hollow cenospheres, which act as stress-distributing inclusions and absorb energy through microcrushing and matrix-filler debonding mechanisms, similarly reported by Pandey et al. [37] in titanium matrix syntactic foams. In contrast, the deformable nature of rubber crumbs allows for energy dissipation via viscoelastic deformation and localized plastic yielding. Studies by Pham et al. [38] on hybrid syntactic foams confirmed that the inclusion of rubber phase improved impact energy absorption by up to 24% compared to traditional microsphere-only systems. When the filler content is increased to 40 vol%, the energy absorption capacity of the cenosphere-based syntactic foam (SFC40) improves by 17.43% to 60.11% compared to SFC20. This enhancement is attributed to the increased density of energy-absorbing cenospheres within the matrix, which provides more sites for energy dissipation through particle crushing and matrix-filler interactions. At the same filler concentration, rubber crumb-based syntactic foams demonstrate even better energy absorption than their cenosphere-based counterparts, with an overall improvement ranging from 7.87% to 23.5%. This superior performance is due to the highly deformable and viscoelastic nature of rubber crumbs, which allows for greater energy absorption and dissipation during impact.

At 60 vol% filler contents, the energy absorption continues to increase for both types of syntactic foams. However, the performance enhancement is more significant in rubber crumb-based foams. The energy absorption values for SFC60 are 3.31 J, 10.73 J, and 11.54 J, whereas for SFR60, they are 4.18 J, 12.43 J, and 16.75 J, respectively, across different impact energy levels. Although higher filler content in cenosphere-based foams enhances energy absorption, it may also introduce increased brittleness, limiting further gains. In contrast, rubber crumb-based foams benefit from rubber's inherent damping characteristics, which lead to better impact resistance. These results confirm that syntactic foams, regardless of the type of filler used, exhibit superior energy absorption capabilities compared to neat epoxy. This enhancement is primarily due to the unique microstructure of syntactic foams, which facilitates efficient energy dissipation upon impact.

All syntactic foam variants consistently outperform their unfilled epoxy counterparts in energy absorption. In the case of cenosphere-reinforced syntactic foams, the inclusion of 60 vol% filler leads to an improvement in energy absorption by approximately 2.37 to 2.59 times compared to neat epoxy, owing to the stiff, lightweight, and crushable nature of cenospheres that contribute to improved impact energy dissipation. A similar trend is observed in rubber crumb-reinforced syntactic foams, where the SFR60 variant shows the highest energy absorption, outperforming both SFR20 and SFR40. Specifically, SFR60 absorbs up to 2.56 times more energy than neat epoxy and 1.77 times more than SFR20. This is a result of multiple synergistic effects: the excellent damping properties of rubber enable energy dissipation through internal friction and viscoelastic deformation; increased rubber content enhances toughness and flexibility; rubber particles serve as microcrack arresters and improve stress distribution; and effective interfacial bonding between rubber and the epoxy matrix ensures efficient transfer and dissipation of impact energy. Together, these factors contribute to a composite system where rubber crumbs provide localized deformation zones for energy absorption, while the epoxy matrix maintains structural integrity and load distribution. The synergy between the rubber and matrix becomes more pronounced with higher rubber content, resulting in significantly improved energy absorption and making rubber crumb-reinforced syntactic foams especially suitable for high-impact applications. At 60 vol%, both filler types continue to improve energy absorption. However, the gains in cenosphere-based foams (SFC60: 3.31 J, 10.73 J, 11.54 J) become less pronounced, potentially due to increased brittleness and filler agglomeration at high loading levels, as also noted by Wang et al. [39] in epoxy-hollow particle systems. In contrast, rubber crumb-based foams at 60 vol.% (SFR60: 4.18 J, 12.43 J, 16.75 J) demonstrate continued enhancement in energy absorption, likely due to more effective stress redistribution and the formation of energy-dissipating microstructures during impact.

The specific energy absorption (SEA) values for neat epoxy are the lowest among all samples, reflecting its limited capacity to absorb and dissipate impact energy effectively, as shown in Figure 8(b). This is consistent with the inherently brittle nature of the epoxy matrix. The incorporation of 20% filler content leads to a noticeable improvement in SEA values for both cenosphere-based (SFC20) and rubber crumb-based (SFR20) syntactic foams, highlighting the positive

influence of fillers on the energy absorption characteristics of the material. Notably, the SEA values of cenosphere-based foams are higher than those of rubber crumb-based foams at the same filler loading. This difference can be attributed to the lower density of cenospheres compared to rubber crumb, resulting in a more favorable mass-to-energy absorption ratio. The presence of cenosphere fillers enhances the material's ability to dissipate energy through mechanisms such as particle crushing and matrix–filler interactions, thereby significantly increasing the SEA values over neat epoxy. In contrast, although rubber crumb fillers contribute to improved energy absorption, the slightly higher density and different material behavior result in lower SEA values compared to cenosphere-based syntactic foams at the same volume fraction. These findings underscore the importance of filler selection, particularly density and mechanical response, in optimizing the specific energy absorption of syntactic foams.

The SEA values indicate that cenosphere-based syntactic foams (SFC20) exhibit superior energy absorption compared to rubber crumb-based syntactic foams (SFR20). This difference is primarily attributed to the density contrast between the two filler types. Cenospheres are low-density, hollow particles that efficiently absorb and distribute impact energy through mechanisms such as crushing and localized deformation. Their low mass contributes to a higher SEA, as more energy is absorbed per unit mass. In contrast, rubber crumbs, while highly deformable and effective in enhancing energy absorption, possess a higher density than cenospheres. As a result, the energy absorbed per unit mass is comparatively lower, leading to slightly reduced SEA values for rubber crumb-based syntactic foams, at higher filler loadings of 40 vol.% and 60 vol.%. A similar trend persists, with cenosphere-reinforced syntactic foams consistently outperforming rubber crumb-reinforced foams in terms of specific energy absorption.

### 3.3 Coefficient of Restitution

In physics, the ratio of the final relative velocities of two objects following a collision to their initial relative velocities, as shown in Eq. 5, is referred to as the coefficient of restitution (COR). It expresses the degree of "bounciness" a collision has. The materials and forms of the objects, as well as the type of impact, all affect the coefficient of restitution. It offers a numerical representation of the amount of kinetic energy retained following impact. A collision with a higher coefficient of restitution is more elastic and conserves more energy, whereas a collision with a lower coefficient of restitution is more inelastic and loses more energy [40], [41].

$$CoR = \frac{v_r}{v_i} \tag{5}$$

where,  $v_r$  and  $v_i$ , respectively, are the residual and starting velocities. The energy loss percentage (ELP) is calculated using Eq. 6

$$ELP = (1 - CoR^2) \times 100 \tag{6}$$

Table 3. CoR and ELP of syntactic foams

Syntactic foams	Energy (J)			Velocity		CoR	ELP
	Impact	Elastic	Absorbed	$V_i$ (m/s)	$V_r$ (m/s)		
NE	39.62	37.86	1.76	3.13	3.05	0.98	4.46
	79.02	74.25	4.77	4.42	4.28	0.97	6.04
	118.82	112.36	6.46	5.42	5.27	0.97	5.44
SFC20	39.62	36.81	2.81	3.13	3.01	0.96	7.11
	79.02	73.65	5.37	4.42	4.26	0.97	6.80
	118.82	111.75	7.07	5.42	5.25	0.97	5.96
SFC40	39.62	36.32	3.30	3.13	2.99	0.96	7.89
	79.02	72.67	6.35	4.42	4.23	0.96	7.88
	118.82	107.5	11.32	5.42	5.15	0.96	7.96
SFC60	39.62	36.31	3.31	3.13	2.99	0.96	8.35
	79.02	68.29	10.73	4.42	4.10	0.96	8.04
	118.82	107.28	11.54	5.42	5.15	0.95	9.53
SFR20	39.62	36.06	3.56	3.13	2.99	0.95	9.00
	79.02	71.94	7.08	4.42	4.22	0.95	8.97
	118.82	104.84	13.98	5.42	5.09	0.94	11.77
SFR40	39.62	36.31	3.31	3.13	3.00	0.96	8.37
	79.02	68.29	10.73	4.42	4.11	0.93	13.58
	118.82	107.28	11.54	5.42	5.15	0.95	9.72
SFR60	39.62	35.44	4.18	3.13	2.96	0.95	10.57
	79.02	66.59	12.43	4.42	4.06	0.92	15.74
	118.82	102.07	16.75	5.42	5.02	0.93	14.10

The computed impact velocity, residual velocity, CoR, and ELP are listed in Table 3. Neat epoxy (NE) has the highest CoR, reflecting the best energy restitution and minimal energy loss, thereby indicating its least efficiency in absorbing the impact energy. Cenosphere reinforced syntactic foams show a gradual decrease in CoR as filler content increases, with the CoR remaining fairly consistent and higher than rubber crumb reinforced syntactic foams. This indicates that rubber crumb SFs are better energy absorbers compared to cenosphere reinforced SFs. Increasing the cenosphere filler content generally results in higher energy absorption but still retains moderate CoR, making it suitable for applications requiring a balance between energy absorption and restitution. Increasing rubber crumb filler content leads to a significant drop in CoR and higher ELP, making these materials better suited for applications where high energy absorption is critical, but energy restitution is less important.

### 3.4 Failure Characterization Analysis

The proposed damage mechanism involving two different types of fillers used to produce syntactic foams is presented in Figure 9. Cenospheres are lightweight, hollow ceramic microspheres predominantly composed of silica ( $\text{SiO}_2$ ) and alumina ( $\text{Al}_2\text{O}_3$ ). These materials impart high compressive strength and low density, making cenospheres suitable for syntactic foam applications in weight-sensitive environments. However, their inherent brittleness, coupled with their thin-walled hollow structure, makes them highly susceptible to failure under impact loading. During low-velocity impacts, the applied stress is not evenly distributed across the material but becomes concentrated at points of contact, particularly around surface imperfections or pre-existing flaws in the cenosphere shell.

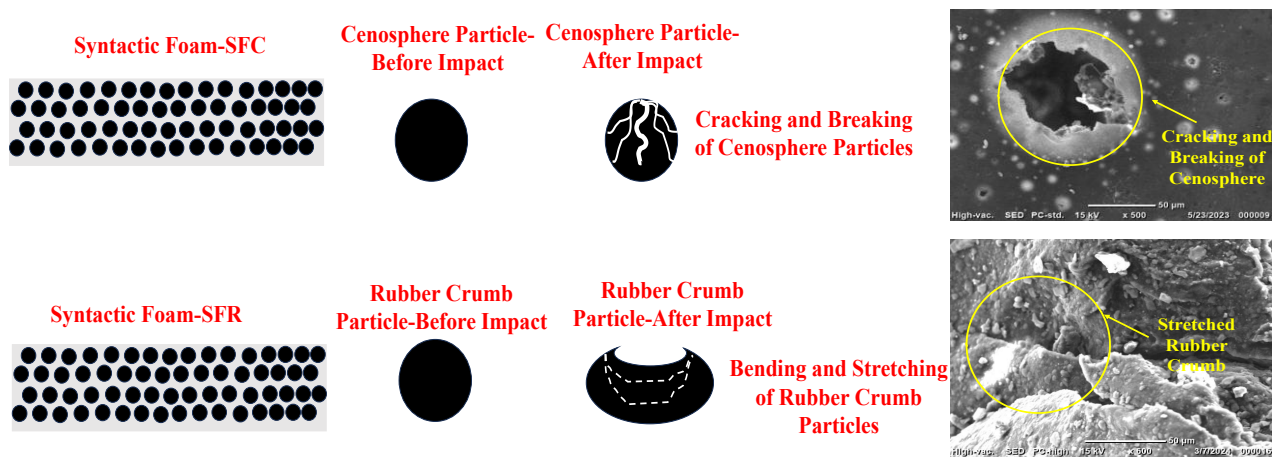


Figure 9. Proposed damage mechanisms involved in SFC and SFR

This stress concentration initiates microcracks on the outer surface of the microsphere. Due to the brittle ceramic nature, these cracks propagate rapidly through the thin wall of the cenosphere without significant plastic deformation. Once a critical stress threshold is surpassed, the cenosphere catastrophically fractures, fragmenting into small shards. This brittle fracture mode is characterized by a sudden release of stored strain energy, leaving behind sharp, angular fragments visible in SEM as signs of shell rupture or particle pull-out. Importantly, brittle materials like cenospheres lack the ability to undergo plastic deformation, which limits their capacity to absorb and dissipate impact energy. Instead of diffusing the energy through material flow or ductile yielding, the majority of the energy is spent on crack initiation and propagation, leading to abrupt failure. As filler volume increases (e.g., in SFC60), the cumulative effect of multiple weak spots from packed cenospheres results in an interconnected network of microcracks, further compromising structural integrity. Thus, while cenospheres contribute to improved stiffness and reduced density, they introduce a mechanically brittle path for failure under impact loading.

In contrast, rubber crumb, obtained from mechanically ground recycled rubber (typically from tires), exhibits hyperelastic behavior, significantly altering the failure dynamics of syntactic foams. Unlike brittle ceramic inclusions, rubber particles can undergo large, reversible deformations under applied stress. When impacted, the energy is initially absorbed through elastic stretching, bending, and compression of the rubber particles, causing a temporary shape change rather than fracture. This energy is stored as strain energy within the molecular structure of the rubber, primarily through elongation of polymer chains. Because of its viscoelastic nature, rubber crumb not only stretches but also exhibits damping behavior, converting part of the impact energy into heat and reducing the amount of energy transmitted through the matrix. Upon unloading, the rubber particles recover their original shape, demonstrating reversible deformation with minimal or no residual damage. Moreover, the flexible rubber phase serves as an internal crack blunter or crack arrestor within the composite. When a propagating crack encounters a rubber crumb, the particle deforms and redistributes the local stress, effectively slowing down or halting crack progression. This contributes to a ductile failure mode where energy is absorbed more gradually, and failure occurs in a more controlled, progressive manner.

At higher filler contents (e.g., in SFR60), rubber crumbs form a more interconnected energy-dissipating network. The result is increased fracture surface roughness and tortuous crack paths, both of which are indicative of higher energy absorption and delayed crack propagation. This morphology is evident in SEM as deep ridges, micro-tearing zones, and

plastic flow features, highlighting a non-catastrophic and highly energy-dissipative failure mechanism. In essence, the brittle fracture behavior of cenospheres makes them suitable for applications where weight reduction and stiffness are prioritized, albeit at the cost of sudden failure under impact. On the other hand, rubber crumb's elastic and energy-dissipative nature makes it ideal for use in protective structures, automotive safety components, or vibration-damping systems, where gradual failure and high energy absorption are desirable. Thus, understanding these contrasting failure mechanisms is crucial for tailoring syntactic foams to specific design criteria and impact resistance requirements.

The fractography of the neat epoxy and foams subjected to the impact test is presented in Figure 10. The failure morphology and energy absorption behavior of syntactic foams are strongly influenced by the type and volume fraction of reinforcements, as clearly evident from the SEM micrographs, as shown in Figure 10 and the corresponding absorbed energy and SEA values presented in Table 2. In the case of neat epoxy (NE), the smooth fracture surface and well-defined river-like crack patterns (Figure 10(a)) point to a typical *brittle fracture mode*, where cracks initiate and propagate rapidly with minimal resistance. The homogeneity of the matrix and lack of any filler-induced crack deflection pathways result in low absorbed energy (6.46 J) and SEA (0.0053 Jm<sup>3</sup>/kg at 118.82 J impact energy). This confirms that NE lacks inherent toughening mechanisms and dissipates negligible energy during failure.

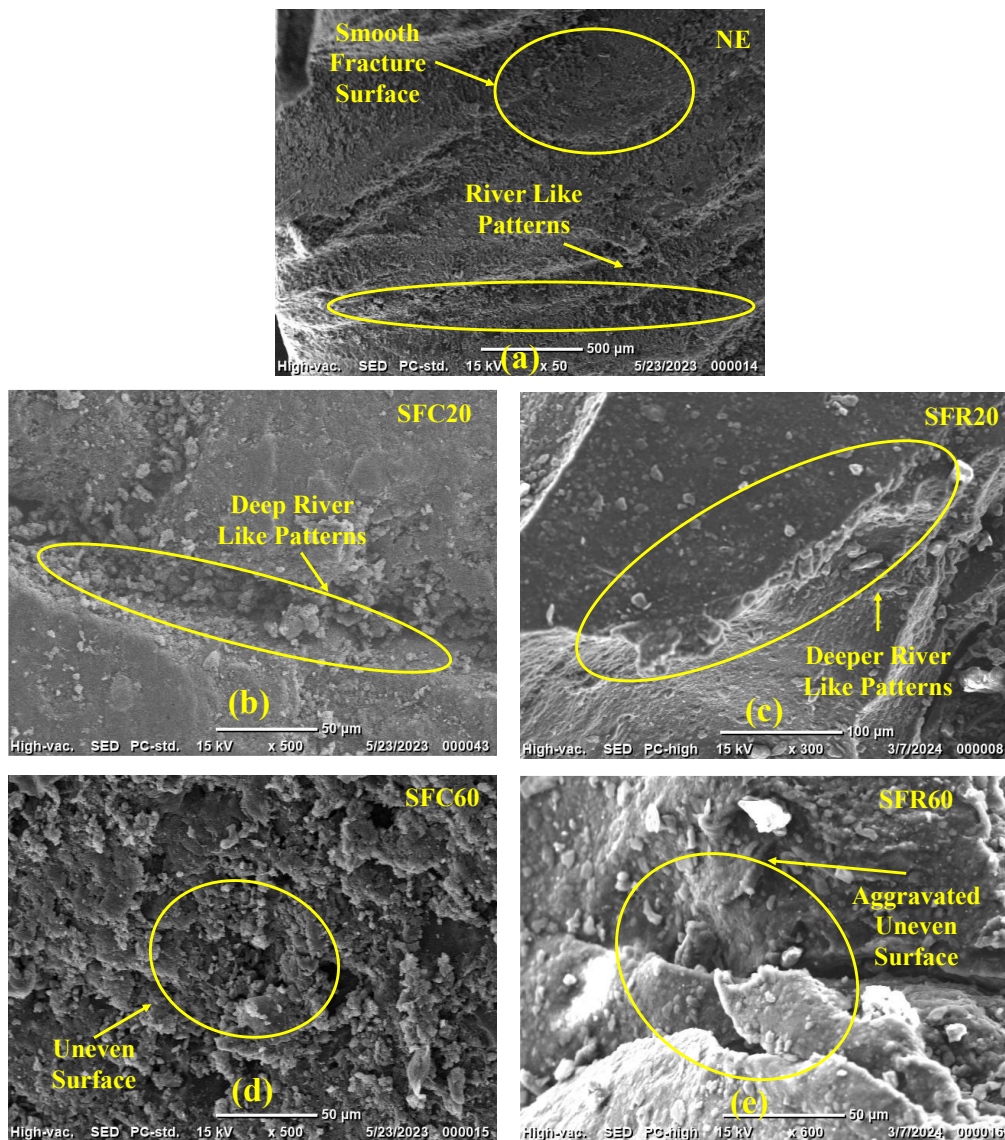


Figure 10. Fractographic analysis of (a) neat epoxy; (b) SFC20; (c) SFR20; (d) SFC60 and (e) SFR60 after impact testing

Upon the incorporation of 20 vol% cenospheres (SFC20), the fracture morphology (Figure 10(b)) transitions to a *semi-brittle mode*, characterized by deeper river-like patterns and the presence of filler-matrix interfaces. The hollow nature of cenospheres introduces microstructural heterogeneities that act as crack arrestors and cause crack deflection or branching. This increased tortuosity in the crack path promotes enhanced frictional energy dissipation and matrix deformation, reflected in the improved absorbed energy (7.07 J) and SEA (0.0063 Jm<sup>3</sup>/kg). However, due to the relatively lower filler content, the extent of matrix toughening remains moderate.

In the case of SFR20 (20 vol% rubber crumb), the SEM image (Figure 10(c)) reveals *ductile–brittle mixed-mode fracture* with deeper and more tortuous river-like features. The rubber crumbs, being elastomeric, contribute to *localized stress relaxation, matrix plastic deformation, and crack blunting*. These mechanisms enhance energy absorption significantly (9.45 J), although the SEA (0.0062 Jm<sup>3</sup>/kg) is slightly lower than SFC20 due to the higher composite density. The ability of rubber particles to elongate and deform under impact provides intrinsic toughening, allowing them to absorb more energy despite not enhancing stiffness.

As the filler content increases to 60 vol%, the material behavior diverges distinctly depending on the reinforcement type. For SFC60, the fracture surface (Figure 10(d)) becomes rough and uneven, with evident signs of *particle agglomeration, interfacial debonding, and void formation*. These phenomena suggest a *brittle fracture mechanism*, exacerbated by poor matrix infiltration and weakened load transfer at high filler concentrations. However, the crack path becomes increasingly tortuous due to the dense filler network, enhancing energy dissipation through microcracking and particle pull-out. This is confirmed by a notable rise in both absorbed energy (11.54 J) and SEA (0.0115 Jm<sup>3</sup>/kg)-the highest among all compositions. Thus, while stiffness and SEA benefit from increased cenospheres, the risk of brittle fracture due to poor interfacial bonding and filler clustering becomes more pronounced.

In stark contrast, SFR60 demonstrates *extensive ductile failure*, as seen in the aggravated uneven surface and fibrillated fracture features (Figure 10(e)). The rubber crumbs facilitate *large-scale matrix deformation, crack meandering, and strain energy absorption*. These effects culminate in the highest absorbed energy recorded (16.75 J at 118.82 J impact energy), although the SEA (0.0103 Jm<sup>3</sup>/kg) is slightly less than that of SFC60 due to higher composite density. The rubber phase at high volume fraction significantly suppresses brittle fracture by promoting mechanisms such as void expansion, crack tip plasticity, and energy dissipation through viscoelastic deformation.

The nature of reinforcement critically dictates the failure mode and energy absorption characteristics. Cenospheres, while enhancing SEA due to their low density and ability to induce crack deflection, can lead to brittle behavior if poorly bonded or agglomerated. Rubber crumbs, on the other hand, offer substantial improvements in total energy absorption through ductile failure mechanisms and matrix toughening, albeit with a trade-off in specific energy absorption due to increased density. Therefore, optimizing filler type and content enables tailored mechanical responses in syntactic foams, balancing stiffness, toughness, and impact resistance for targeted structural applications.

#### 4. CONCLUSIONS

This study successfully developed syntactic foams reinforced with cenospheres (SFC) and rubber crumb (SFR) and investigated their low-velocity impact response. Both types of foams demonstrated improved energy absorption compared to neat epoxy (NE), with performance increasing alongside filler content and impact energy. At 20%, 40%, and 60% filler levels, SFR foams absorbed 11–33.66% more energy than SFC foams, highlighting the superior energy dissipation capability of rubber crumb. However, SFC foams consistently exhibited higher specific energy absorption (SEA), with SFC60 achieving the highest SEA of 0.0115 Jm<sup>3</sup>/Kg at 118.82 J, making it optimal for weight-sensitive impact applications. Fracture surface analysis further supported these findings, revealing increased surface roughness and complexity with higher filler content. SFR foams, particularly SFR60, exhibited deeper and more irregular fracture topography, indicating higher fracture energy absorption. In contrast, pure epoxy showed a smooth and brittle fracture.

Overall, SFC foams are preferable when a balance between weight and energy absorption is critical, whereas SFR foams are more suitable for applications requiring maximum energy dissipation. These findings underscore the potential of both filler systems in enhancing the impact resistance of polymer composites for structural and protective applications. From a design perspective, SFC foams are recommended for applications where low weight and moderate energy absorption must be balanced, such as drones, satellite panels, or portable enclosures. In contrast, SFR foams are more suitable for shock mitigation and protective structures, including helmets, automotive bumpers, and packaging materials, where maximum energy dissipation is essential. Furthermore, the use of waste-derived fillers like cenospheres (from fly ash) and rubber crumb (from end-of-life tires) contributes to material sustainability and circular economy goals, making these composites environmentally and economically attractive for structural and protective engineering applications.

#### ACKNOWLEDGEMENTS

The author would like to acknowledge the support of SERB, New Delhi, India for providing financial assistance through TARE/2021/000016.

#### CONFLICT OF INTEREST

The authors declare no conflicts of interest.

#### AUTHORS CONTRIBUTION

Vishwas Mahesh-Conceptualisation; Methodology; Formal analysis; Investigation; Resources; Writing - original draft; Writing - review & editing; Funding acquisition; Project administration.

## REFERENCES

- [1] M. Rafiquzzaman, M. Taimum Islam, M. Raihan Hossain, M. Fazla Rabby, and M. Rifat Hashar, "Fabrication and performance test of glass-bamboo fiber based industry safety helmet," *American Journal of Mechanical and Materials Engineering*, vol. 1, no. 1, pp. 20–25, 2017.
- [2] V. Mahesh, V. Mahesh, P. Hadi, and D. Harursampath, "An investigation into low - velocity impact behavior of functionally graded treated and untreated cenosphere - based syntactic foams," *Journal of the Brazilian Society of Mechanical Sciences and Engineering*, vol. 46, no. 3, p. 170. 2024.
- [3] B. Shivamurthy, Siddaramaiah, and M. S. Prabhushwamy, "Influence of SiO<sub>2</sub> fillers on sliding wear resistance and mechanical properties of compression moulded glass epoxy composites," *Journal of Minerals and Materials Characterization and Engineering*, vol. 8, no. 7, pp. 513–530, 2009.
- [4] A. Satapathy, A. Kumar Jha, S. Mantry, S. K. Singh, and A. Patnaik, "Processing and characterization of jute-epoxy composites reinforced with SiC derived from rice husk," *Journal of Reinforced Plastics and Composites*, vol. 29, no. 18, pp. 2869–2878, 2010.
- [5] V. Mahesh, V. Mahesh, S. M. Nagaraj, P. Subhashaya, and G. S. T. Shambu Singh, "Physio-mechanical and thermal characterization of jute/rubber crumb hybrid composites and selection of optimal configuration using the MADM approach," *Proceedings of the Institution of Mechanical Engineers, Part C: Journal of Mechanical Engineering Science*, vol. 236, no. 14, pp. 7942–7952, 2022.
- [6] V. Mahesh, V. Mahesh, D. Harursampath, S. Joladarashi, and S. M. Kulkarni, "Development of sustainable jute/epoxy composite and assessing the effect of rubber crumb on low velocity impact response," *Journal of Natural Fibers*, vol. 19, no. 15, pp. 12268–12279, 2022.
- [7] S. Chandrika, T. R. H. Kumar, and V. Mahesh, "Physio-mechanical characterization of kenaf/saw dust reinforced polymer matrix composite and selection of optimal configuration using MADM-VIKOR approach," *International Journal on Interactive Design and Manufacturing*, vol. 18, no. 9, pp. 6359–6369, 2022.
- [8] M. Vishwas, M. Vinyas, and K. Puneeth, "Influence of areca nut nanofiller on mechanical and tribological properties of coir fibre reinforced epoxy-based polymer composite," *Scientia Iranica*, vol. 27, no. 4, pp. 1972–1981, 2020.
- [9] V. Mahesh, "Development and physio-mechanical characterization of sustainable jute-wood dust reinforced hybrid composites," *Journal of Natural Fibers*, vol. 19, no. 16, pp. 13995–14004, 2022.
- [10] C. Qi, F. Jiang, A. Remennikov, L. Z. Pei, J. Liu, J. S. Wang, et al., "Quasi-static crushing behavior of novel re-entrant circular auxetic honeycombs," *Composites Part B: Engineering*, vol. 197, p. 108117, 2020.
- [11] M. S. Sreekanth, V. A. Bambole, S. T. Mhaske, and P. A. Mahanwar, "Effect of particle size and concentration of flyash on properties of polyester thermoplastic elastomer composites," *Journal of Minerals and Materials Characterization and Engineering*, vol. 8, no. 3, pp. 237–248, 2009.
- [12] V. A. Prabu, R. D. J. Johnson, P. Amuthakkannan, and V. Manikandan, "Usage of industrial wastes as particulate composite for environment management: Hardness, tensile and impact studies," *Journal of Environmental Chemical Engineering*, vol. 5, no. 1, pp. 1289–1301, 2017.
- [13] K. Pal, R. Rajasekar, D. J. Kang, Z. X. Zhang, S. K. Pal, C. K. Das, et al., "Effect of filler and urethane rubber on NR/BR with nanosilica: Morphology and wear," *Journal of Thermoplastic Composite Materials*, vol. 23, no. 5, pp. 717–739, 2010.
- [14] S. Biswas and A. Satapathy, "A comparative study on erosion characteristics of red mud filled bamboo–epoxy and glass–epoxy composites," *Materials & Design*, vol. 31, no. 4, pp. 1752–1767, 2010.
- [15] N. Chand, P. Sharma, and M. Fahim, "Correlation of mechanical and tribological properties of organosilane modified cenosphere filled high density polyethylene," *Materials Science and Engineering A*, vol. 527, no. 21, pp. 5873–5878, 2010.
- [16] P. R. Pati and A. Satapathy, "Prediction and simulation of wear response of Linz-Donawitz (LD) slag filled glass-epoxy composites using neural computation," *Polymers for Advanced Technologies* vol. 26, no. 2, pp. 121–127, 2015.
- [17] V. Mahesh, "Advanced cenosphere-reinforced syntactic foams: focus on specific strength enhancement," *Iranian Polymer Journal*, pp. 1-16, 2024.
- [18] N. Ayrilmis, A. M. Kuzmin, T. Masri, M. Yagoub, L. Sedira, P. Pantyukhov, et al., "Effects of reinforcement by both waste glass and barley straw on water resistance, mechanical, and thermal properties of polyethylene composite," *BioResources*, vol. 20, no. 3, pp. 5967–5987, 2025.
- [19] D. Bachtiar, A. A. Mohammed, S. Palanisamy, A. I. Imran, J. P. Siregar, M. R. Mat Rejab, et al., "Effect of alkaline treatment on the thermal and mechanical properties of sugar palm fibre reinforced thermoplastic polyurethane composites," *Scientific Reports*, vol. 15, no. 1, p. 14085, 2025.

- [20] M. Doddamani and S. Kulkarni, "Dynamic response of fly ash reinforced functionally graded rubber composite sandwiches - A Taguchi approach," *International Journal of Engineering Science and Technology*, vol. 3, no. 1, pp. 166–182, 2011.
- [21] K. Shahapurkar, "Compressive behavior of crump rubber reinforced epoxy composites," *Polymer Composites*, vol. 42, no. 1, pp. 329–341, 2021.
- [22] N. Gupta and E. Woldesenbet, "Microscopic studies of syntactic foams tested under three-point bending conditions," in *Engineering Technology Conference on Energy*, Texas, USA: ASME, 2009, pp. 147–152.
- [23] N. Gupta, R. Ye, and M. Porfiri, "Comparison of tensile and compressive characteristics of vinyl ester/glass microballoon syntactic foams," *Composites Part B: Engineering*, vol. 41, no. 3, pp. 236–245, 2010.
- [24] F. N. Linhares, C. F. S. Gabriel, A. Maria, F. De Sousa, R. Céilia, and R. Nunes, "Applied clay science mechanical and rheological properties of nitrile rubber / fluoromica composites," *Applied Clay Science*, vol. 162, pp. 165–174, 2018.
- [25] R. Ibrahim, "Effect of date palm seeds on the tribological behaviour of polyester composites under different testing conditions," *Journal of Materials Science: Materials in Engineering*, vol. 4, no. 6, p. 1000206, 2015.
- [26] V. Mahesh, V. Mahesh, D. Harursampath, J. Shivanna, R. C. Lakshmikanth, G. T. Renukumar, et al., "Three body abrasion wear resistance of cenosphere particle-reinforced syntactic foams developed using molding method," *Polymer Engineering & Science*, vol. 63, no. 9, pp. 3091–3104, 2023.
- [27] S. Thakur and S. R. Chauhan, "Friction and sliding wear characteristics study of submicron size cenosphere particles filled vinylester composites using Taguchi design of experimental technique," *Journal of Composite Materials*, vol. 48, no. 23, pp. 2831–2842, 2014.
- [28] P. R. Pati and M. P. Satpathy, "Effect of process parameters on sliding wear performance of red brick dust-filled glass-epoxy composites," *Proceedings of the Institution of Mechanical Engineers, Part J: Journal of Engineering Tribology*, vol. 236, no. 9, pp. 1846–1854, 2022.
- [29] P. R. Pati and M. P. Satpathy, "Investigation on red brick dust filled epoxy composites using ant lion optimization approach," *Polymer Composites*, vol. 40, no. 10, pp. 3877–3885, 2019.
- [30] V. V. Mahesh, S. Joladarashi, and S. M. Kulkarni, "Comparative study on energy absorbing behavior of stiff and flexible composites under low velocity impact," *Proceedings of the Second International Conference on Polymer Composites* vol. 2057, p. 020025, 2019.
- [31] A. Ali Emadi and A. Modarres, "Impact of crumb rubber particles on the fracture parameters of concrete through WFM, SEM and BEM," *Construction and Building Materials*, vol. 305, p. 124693, 2021.
- [32] M. R. Doddamani and S. M. Kulkarni, "Response of fly ash-reinforced functionally graded rubber composites subjected to mechanical loading," *Mechanics of Composite Materials*, vol. 48, no. 1, pp. 89–100, 2012.
- [33] P. K. Rohatgi, N. Gupta, B. F. Schultz, and D. D. Luong, "The synthesis, compressive properties, and applications of metal matrix syntactic foams," *Jom*, vol. 63, no. 2, pp. 36–42, 2011.
- [34] Y. Zhao and D. Drummer, "Influence of filler content and filler size on the curing kinetics of an epoxy resin," *Polymers (Basel)*, vol. 11, no. 11, p.1797, 2019.
- [35] K. T. Tan, N. Watanabe, and Y. Iwahori, "Effect of stitch density and stitch thread thickness on low-velocity impact damage of stitched composites," *Composites Part A: Applied Science and Manufacturing*, vol. 41, no. 12, pp. 1857–1868, 2010.
- [36] V. Mahesh, V. Mahesh, and D. Harursampath, "On low velocity impact response of Sandwich composite with jute/epoxy facesheet and cenosphere reinforced functionally graded Core: Experimental and finite element approach," *Polymer Composites*, vol. 45, no. 14, pp. 13151–13163, 2024.
- [37] S. Pandey, A. N. C. Venkat, D. P. Mondal, J. D. Majumdar, A. K. Jha, H. Rao, et al., "Effect of cenosphere size and volume fraction on the microstructure and deformation behavior of ti-cenosphere syntactic foam made through powder metallurgy route," *Materials Performance and Characterization*, vol. 5, no. 1, pp. 266–288, 2016.
- [38] A. J. Satti, R. Quijada, J. M. Pastor, and E. M. Vallés, "Morphological Raman analysis of short chain branched ethylene and propylene metallocenic copolymers," *Polymer Testing*, vol. 67, pp. 450–456, 2018.
- [39] H. Wang, R. Yan, H. Cheng, M. Zou, H. Wang, and K. Zheng, "Hollow glass microspheres/phenolic syntactic foams with excellent mechanical and thermal insulate performance.," *Frontiers in Chemistry*, vol. 11, p. 1216706, 2023.
- [40] A. Aryaei, K. Hashemnia, and K. Jafarpur, "Experimental and numerical study of ball size effect on restitution coefficient in low velocity impacts," *International Journal of Impact Engineering*, vol. 37, no. 10, pp. 1037–1044, 2010.
- [41] A. Chatterjee, *Rigid body collisions: Some general considerations, new collision laws and some experimental data*, Cornell University, 1997.